

First redshift determination of an optically/UV faint submillimeter galaxy using CO emission lines

A. Weiß¹, R. J. Ivison^{2,3}, D. Downes⁴, F. Walter⁵, M. Cirasuolo^{2,3}, K. M. Menten¹

ABSTRACT

We report the redshift of a distant, highly obscured submm galaxy (SMG), based entirely on the detection of its CO line emission. We have used the newly commissioned Eight-Mixer Receiver (EMIR) at the IRAM 30m telescope, with its 8 GHz of instantaneous dual-polarization bandwidth, to search the 3-mm atmospheric window for CO emission from SMM J14009+0252, a bright SMG detected in the SCUBA Lens Survey. A detection of the CO(3–2) line in the 3-mm window was confirmed via observations of CO(5–4) in the 2-mm window. Both lines constrain the redshift of SMM J14009+0252 to $z = 2.9344$, with high precision ($\delta z = 2 \cdot 10^{-4}$). Such observations will become routine in determining redshifts in the era of the Atacama Large Millimeter/submillimeter Array (ALMA).

Subject headings: cosmology: observations — galaxies: evolution — galaxies: high-redshift — galaxies: starburst — ISM: molecules

1. Introduction

Sensitive blank-field mm and submm continuum surveys have discovered hundreds of dusty, star-forming submm galaxies (SMGs) over the past decade (e.g. Smail, Ivison & Blain 1997; Barger et al. 1999; Borys et al. 2003; Greve et al. 2004; Coppin et al. 2006). Determining their redshift distribution has been much slower, however, because the large dust content of SMGs means that they often have only weak (if any) counterparts in the rest-frame ultraviolet and optical, making spectroscopic redshift determinations extremely difficult (e.g. Smail et al. 2002; Dannerbauer et al. 2002). Furthermore, the poor spatial resolution of mm/submm continuum sur-

veys (typically 11–19'') means that several potential, faint optical/near-IR counterparts exist. This requires deep radio or *Spitzer* mid-IR images to pinpoint the most likely counterpart for optical spectroscopic follow-up observations (e.g. Ivison et al. 2002, 2004). The largest SMG redshift survey published so far was based on radio-identified SMGs (Chapman et al. 2005), which may bias the redshift distribution since radio emission may remain undetected even in the deepest radio maps for sources at $z > 3$.

A promising alternative route to determine the redshift of an SMG is through observations of CO emission lines at cm or mm wavelengths. These lines arise from the molecular gas, the fuel for star formation and can thus be related unambiguously to the submm continuum source. Therefore, these observations do not require any additional multi-wavelength identification and circumvent many of the problems inherent to optical spectroscopy of SMGs.

The narrow bandwidth of existing mm receivers, however, placed severe limitations on this approach as it was too time-consuming to search blindly for the CO lines in redshift space via multiple frequency tunings. In recent years,

¹Max-Planck Institut für Radioastronomie, Auf dem Hügel 69, 53121 Bonn, Germany

²UK Astronomy Technology Centre, Royal Observatory, Blackford Hill, Edinburgh, EH9 3HJ, UK

³Institute for Astronomy, University of Edinburgh, Royal Observatory, Blackford Hill, Edinburgh, EH9 3HJ, UK

⁴Institut de Radio Astronomie Millimetrique, 300 Rue de la Piscine, Domaine Universitaire, 38406 Saint Martin d'Hères, France

⁵MPIA, Königstuhl 17, 69117 Heidelberg, Germany

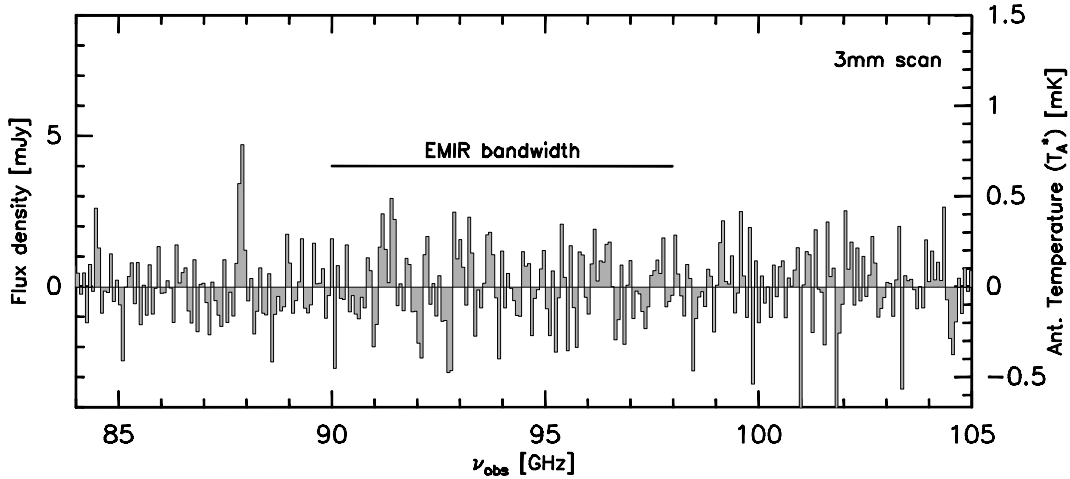


Fig. 1.— 20-GHz-wide spectral scan at a velocity resolution of 200 km s^{-1} towards SMM J14009+0252 in the 3-mm window. A CO emission feature is seen at $\sim 88 \text{ GHz}$ (see Fig. 2 for a presentation of the CO line at higher spectral resolution).

a lot of effort has been invested in overcoming this bandwidth limitation at various radio facilities (e.g. Naylor et al. 2003; Erickson et al. 2007; Harris et al. 2007). With the commissioning of the multi-band heterodyne receiver, EMIR, at the IRAM 30 m telescope, this situation has greatly improved. EMIR’s 8-GHz instantaneous, dual-polarization bandwidth in the 3-mm band provides the same spectral coverage as ALMA. Combined with the large collecting area of the 30 m telescope this allows for blind searches for high-redshift CO lines at mm wavelengths.

To demonstrate the capabilities of EMIR as a ‘redshift machine’, we targeted SMM J14009+0252. This source was discovered by the Submillimeter Common User Bolometer Array (SCUBA) in early 1998 and is one of the brightest SMGs discovered to date ($S_{850\mu\text{m}} = 15.6 \text{ mJy}$, Ivison et al. 2000). Despite several attempts, and the availability of an accurate radio position, no spectroscopic redshift could be determined – mainly because of its faintness at near-IR/optical wavelengths. In this letter we report the results of our blind search for CO lines in this SMG.

2. Observing Strategy

The 3-mm (E090) set-up of EMIR provides 8 GHz of instantaneous, dual-polarization bandwidth. The entire accessible frequency range,

83 – 117 GHz, can be covered with five tunings. This corresponds to $0 < z < 0.4$ for CO(1–0) and $1.0 < z < 8.7$ for the CO lines between ($J = 2 - 1$) and (7–6), with only a small gap at $1.78 < z < 1.98$. The gap can be covered by 2-mm observations, i.e. EMIR is a powerful instrument to search for high-redshift ($z > 1$) CO emission.

Observations were made in July 2009 during average summer conditions ($\sim 7 \text{ mm}$ precipitable water vapor). Data were recorded using 16 units of the Wideband Line Multiple Autocorrelator (WILMA, 1 GHz of bandwidth each) to cover 8 GHz in both polarizations. WILMA provides a spectral resolution of 2 MHz which corresponds to $5\text{--}7 \text{ km s}^{-1}$ for the 3-mm band. The observations were done in wobbler-switching mode, with a switching frequency of 1 Hz and an azimuthal wobbler throw of $100''$. Pointing was checked frequently on the nearby quasar J1226+023 and was found to be stable to within $3''$. Calibration was done every 12 min using the standard hot/cold-load absorber. The data were processed with the CLASS software. We omitted scans with distorted baselines and subtracted only linear baselines from individual spectra.

We first scanned the full 3-mm tuning range of EMIR with $\sim 2 \text{ hr}$ of observing for each tuning. The tunings were spaced to provide 500 MHz overlap. Excellent receiver noise temperatures across the band (35–45 K) resulted in typical system tem-

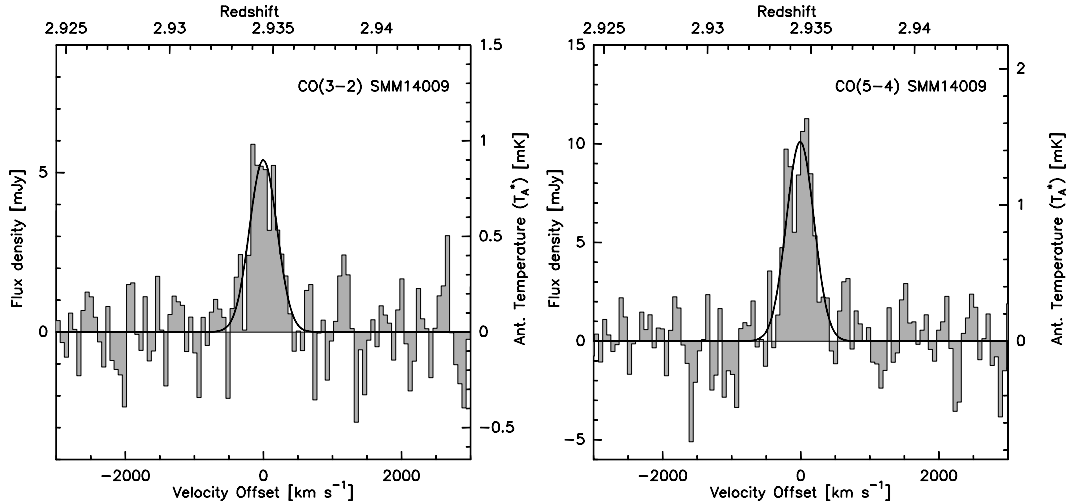


Fig. 2.— Spectra of the CO(3–2) (left) and CO(5–4) (right) lines towards SMM J14009+0252. The spectral resolution is 60 km s^{-1} for both lines. See Table 1 for the fit parameters.

peratures of $\sim 100 \text{ K}$. The resulting spectrum had an r.m.s. noise level of 0.5 mK ($\approx 3.5 \text{ mJy}$) at a velocity resolution of 200 km s^{-1} but did not show clear evidence for CO line emission. We then increased the integration time for the lower part ($< 105 \text{ GHz}$) of the 3-mm band until we reached an average r.m.s. noise level of 0.2 mK (1.2 mJy). The resulting spectrum, shown in Fig. 1, shows a line at $\sim 88 \text{ GHz}$.

At this stage the source redshift was still not determined as it was not clear which CO transition was detected in the 3-mm scan. We therefore used the dual-frequency 3-/2-mm (E090/E150) set-up of EMIR to search for a second CO transition in the 2-mm band and to increase the signal-to-noise ratio of the 3-mm line. In this configuration, each frequency band has an instantaneous, dual-polarization bandwidth of 4 GHz . The 2-mm mixers were tuned to 146.5 GHz , under the assumption that the 3-mm line was the CO(3–2) transition at $z = 2.93$. At this frequency the receiver noise temperature was $\sim 30 \text{ K}$, yielding a system temperature of $\sim 120 \text{ K}$. SMM J14009+0252 was observed in the dual-frequency set-up for $\sim 5 \text{ hr}$ and we clearly detected a second line in the 2-mm band (see Fig. 2). Additional 2-mm data were taken in an attempt to observe a third CO line in the 1-mm band (E150/E230 configuration). Given the relatively poor observing conditions, the 1-mm data did not yield a meaningful limit.

The beam sizes/antenna gains for the line frequencies at 3 and 2 mm are $28''/6.0 \text{ Jy K}^{-1}$ and $15''/6.5 \text{ Jy K}^{-1}$, respectively. We estimate the flux density scale to be accurate to $\pm 10\text{--}15\%$.

3. Results

The final 3- and 2-mm spectra are shown at a velocity resolution of 60 km s^{-1} in Fig. 2. The r.m.s. noise level (T_A^*) for both spectra is $160 \mu\text{K}$ (1.0 mJy) and $180 \mu\text{K}$ (1.3 mJy) at 3 and 2 mm, respectively. Both lines are detected at high significance (9 and 12σ for the integrated intensities). The line profiles for both lines are very similar and well described by a single Gaussian with a FWHM of 470 km s^{-1} . The parameters derived from Gaussian fits to both line profiles are given in Table 1. The frequencies unambiguously identify the lines as CO(3–2) and CO(5–4) (see our discussion below). Combining the centroids of both lines, we derive a variance-weighted mean redshift for SMM J14009+0252 of $z = 2.9344 \pm 2 \cdot 10^{-4}$.

4. Discussion

At first glance the observed frequencies can not only be interpreted as CO(3–2) and CO(5–4) at $z = 2.93$ but also as CO(6–5) and CO(10–9) at $z = 6.88$ or even CO(9–8) and CO(15–14) at $z = 10.80$. The CO ladder, however, is not equidistant in frequency which results in small,

TABLE 1
CO LINE PARAMETERS FOR SMM J14009+0252.

Line	ν_{obs} [GHz]	z_{CO}	S_ν [mJy]	ΔV [km s ⁻¹]	I [Jy km s ⁻¹]	$L' \text{ }^{a,b}$ [10 ¹⁰ K km s ⁻¹ pc ²]	$L \text{ }^{a,b}$ [10 ⁷ L_\odot]
CO(3-2)	87.888(8)	2.93450(35)	5.4 ± 0.9	470 ± 60	2.7 ± 0.3	7.9 ± 0.9	10.4 ± 1.2
CO(5-4)	146.469(9)	2.93438(26)	10.2 ± 1.3	472 ± 45	5.1 ± 0.4	5.3 ± 0.4	32.7 ± 2.7

^acorrected for a lens magnification of $m = 1.5$ (Ivison et al. 2000)

^bAdopted luminosity distance: 25.16 Gpc; angular size distance: 1.625 Gpc; linear scale: 7.879 kpc/'' (for $H_0 = 71 \text{ km s}^{-1} \text{ Mpc}^{-1}$, $\Omega_\Lambda = 0.73$ and $\Omega_M = 0.27$ (Spergel et al. 2003))

but significant differences for the frequency separation of the line-pairs as a function of rotational quantum number. The frequency separation is 58.577, 58.532 and 58.458 GHz for the CO line-pairs at redshifts 2.93, 6.88 and 10.80, respectively. Our observations yield $\delta\nu = 58.581 \pm 0.017$ GHz which identifies the lines as CO(3-2) and CO(5-4) at $z = 2.93$. Our redshift confirms earlier photometric redshift estimates by Ivison et al. (2000, $z > 2.8$ based on S_{450}/S_{850} and $3 < z < 5$ based on the whole spectral energy distribution (SED)), Yun & Carilli (2002, $z \sim 3.5$ based on the dust SED) and more recently by Hempel et al. (2008, $z = 2.8 - 3$ based on optical/IR photometry).

With the precise redshift and the observed CO line luminosities in hand we can estimate the molecular gas content of SMM J14009+0252. The observed CO(5-4) to CO(3-2) line ratio (0.7) implies that the CO emission is sub-thermally excited, at least for the CO(5-4) line. This line ratio is identical to that observed for SMM J16359+6612 (Weiß et al. 2005) and we employ the large velocity gradient models discussed in that paper to estimate a CO(1-0) line luminosity of $L' \approx 8.2 \cdot 10^{10} \text{ K km s}^{-1} \text{ pc}^2$. This translates into a molecular gas mass of $M_{\text{H}_2} \approx 6.5 \cdot 10^{10} M_\odot$ using a standard ULIRG conversion factor of $0.8 M_\odot (\text{K km s}^{-1} \text{ pc}^2)^{-1}$ (Downes & Solomon 1998). These numbers take the lens magnification of $m = 1.5$ due to the foreground cluster, Abell 1835 at $z = 0.25$, into account (Ivison et al. 2000).

The large molecular gas mass is in line with estimates based on the dust continuum measurements. The 1350-, 850- and 450- μm observations (see Ivison et al. 2000, for a compilation of the

observed flux densities) can be described by a dust temperature of ~ 40 K (similar to the kinetic temperature of the CO model) and a gas mass of $M_{\text{H}_2} \approx 8 \cdot 10^{10} M_\odot$ using the dust model in Weiß et al. (2007) and a gas-to-dust mass ratio of 100. The implied far-IR luminosity (integral between 40-120 μm , Helou et al. (1985)) of this model is $\approx 3 \cdot 10^{12} L_\odot$ which corresponds to a star-formation rate of $\approx 500 M_\odot \text{ yr}^{-1}$. These numbers classify SMM J14009+0252 as a ULIRG.

We note, however, that this model underestimates the observed 24- μm flux density and additional warmer dust components are required to fit the mid-IR data (see Fig. 3). Such a multi-component dust model predicts $L_{\text{FIR}} \approx 4 - 5 \cdot 10^{12} L_\odot$, although the lack of data between 24 and 450 μm means that the shape of the Wien tail of the dust SED is not well constrained. In any case the estimated far-IR luminosity is far ($\sim \times 5$) lower than estimates based on the radio/far-IR correlation (Condon 1992) which supports the conclusion of Ivison et al. (2000) that SMM J14009+0252 contains a radio-loud active galactic nucleus.

We thank the IRAM telescope operators for their support during the observations. IRAM is supported by INSU/CNRS (France), MPG (Germany) and IGN (Spain).

REFERENCES

- Barger, A.J., Cowie, L.L., Sanders, D.B., 1999, ApJ, 518, 5
Borys, C., Chapman, S.C., Halpern, M., Scott, D., 2003, MNRAS, 334, 385

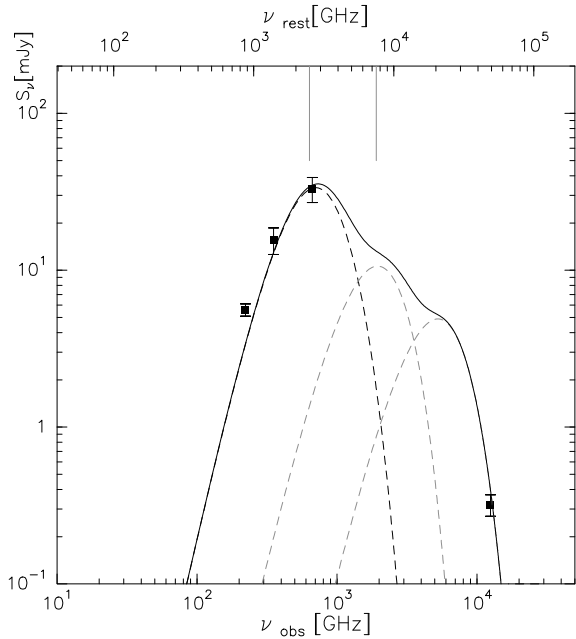


Fig. 3.— Dust SED towards SMM J14009+0252. The black and the two grey dotted lines show a 40, 75 and 200 K dust component, respectively. The far-IR luminosity of this model is $3.8 \cdot 10^{12} L_{\odot}$. The solid grey lines at the top indicate the rest-frame 40-120 μm integration limits used to compute the far-IR luminosity.

Chapman, S.C., Blain, A.W., Smail, I., & Ivison, R.J. 2005, *ApJ*, 622, 772

Condon, J.J. 1992, *ARA&A*, 30, 575

Coppin, K., et al. 2006, *MNRAS* 372, 1621

Dannerbauer, H., Lehnert, M.D., Lutz, D., Tacconi, L., Bertoldi, F., Carilli, C., Genzel, R., Menten, K. 2002 *ApJ*, 573, 473

Downes, D., & Solomon, P.M. 1998, *ApJ*, 507, 615

Erickson, N., Narayanan, G., Goeller, R., & Grosslein, R. 2007, *ASPC*, 375, 71

Greve, T.R., Ivison, R.J., Bertoldi, F., et al. 2004, *MNRAS*, 354, 779

Harris, A.I., et al. 2007 *ASPC*, 375, 82

Helou, G., Soifer, B.T., & Rowan-Robinson, M. 1985, *ApJ*, 298, 7

Hempel, A., Schaerer, D., Egami, E., Pelló, R., Wise, M., Richard, J., Le Borgne, J.F., & Kneib, J.P. 2008, *A&A*, 477, 55

Ivison, R.J., Smail, Ian, Barger, A.J., Kneib, J.-P., Blain, A.W., Owen, F.N., Kerr, T.H. & Cowie, L.L. 2000, *MNRAS*, 315, 209

Ivison, R.J. et al. 2002, *MNRAS*, 337, 1

Ivison, R.J., Greve, T.R., Serjeant, S. et al. 2004 *ApJS*, 154, 124

Naylor, B.J., et al. 2003, *SPIE*, 4855, 239

Smail, I., Ivison, R.J., & Blain, A.W., 1997, *ApJ*, 490, 5

Smail, I., Ivison, R.J., Blain, A.W., & Kneib, J.P. 2002, *MNRAS*, 331, 495

Spergel, D.N., et al. 2003, *ApJS*, 148, 175

Weiß, A., Downes, D., Walter, F., & Henkel, C. 2005 *A&A*, 440, 45

Weiß, A., Downes, D., Neri, R., Walter, F., Henkel, C., Wilner, D.J., Wagg, J., Wiklind, T. 2007 *A&A*, 467, 955

Yun, M.S., & Carilli, C.L. 2002, *ApJ*, 568, 88

This 2-column preprint was prepared with the AAS L^AT_EX macros v5.2.